

## Modified bimodal growth mechanism of pentacene thin films at elevated substrate temperatures

This article has been downloaded from IOPscience. Please scroll down to see the full text article.

2010 J. Phys.: Condens. Matter 22 262001

(<http://iopscience.iop.org/0953-8984/22/26/262001>)

View [the table of contents for this issue](#), or go to the [journal homepage](#) for more

Download details:

IP Address: 129.252.86.83

The article was downloaded on 30/05/2010 at 08:52

Please note that [terms and conditions apply](#).

## FAST TRACK COMMUNICATION

# Modified bimodal growth mechanism of pentacene thin films at elevated substrate temperatures

Dong Guo<sup>1,2,3</sup>, Susumu Ikeda<sup>2</sup> and Koichiro Saiki<sup>2</sup>

<sup>1</sup> Institute of Acoustics, Chinese Academy of Sciences, Bei-Si-Huan-Xi Road 21, Beijing 100190, People's Republic of China

<sup>2</sup> Department of Complexity Science and Engineering, Graduate School of Frontier Sciences, The University of Tokyo, Kashiwanoha 5-1-5, Kashiwa, Chiba, Japan

E-mail: [dong.guo@mail.ioa.ac.cn](mailto:dong.guo@mail.ioa.ac.cn)

Received 6 April 2010, in final form 26 April 2010

Published 24 May 2010

Online at [stacks.iop.org/JPhysCM/22/262001](http://stacks.iop.org/JPhysCM/22/262001)

## Abstract

The growth of pentacene thin films at elevated temperatures was studied. We observed decreased grain size and crystallinity with increasing substrate temperature in 30 nm films, despite the increased grain size of the submonolayer films. These were attributed to a two-dimensional to three-dimensional growth transition and a pronounced desorption of the first monolayer molecules. The observed coarsening-like behavior and the dendritic to compact grain geometry transition with temperature were explained by classic growth theories. A modified bimodal growth mechanism at elevated temperatures was proposed by analyzing both the out-of-plane and the in-plane grazing incidence x-ray diffraction patterns of the same films.

(Some figures in this article are in colour only in the electronic version)

## 1. Introduction

Organic semiconductors based on conjugated polymers, oligomers, or other molecules have received considerable attention due to their importance in fundamental physics and potential application in flexible electronics. The realization that the performance of the relevant devices is inherently associated with the quality of the organic thin films has stimulated numerous studies in organic semiconductor growth. However, due to the specific nature of large size, anisotropy and relatively weak van der Waals interaction of organic molecules, their growth is much more complex than that of inorganic materials, and the physical principles are still not well established. Pentacene has been recognized as a model small-molecule organic semiconductor due to its high carrier charge mobility [1]. While significant progress has been made in understanding the growth physics of pentacene films [1–7], the exact role of different deposition parameters in controlling

the morphology and structure of the vacuum deposited films remains poorly understood. Particularly, substrate temperature ( $T_s$ ) has a complicated influence on the pentacene growth, since the many thermally activated competing processes may cause nucleation of the 'bulk phase' [5–7], surface diffusion limits, and formation of defects. Actually, although the grain size and crystallinity are generally expected to increase with increasing  $T_s$  [1, 8], rather different results of increased [9], decreased [10] and unchanged [11] charge carrier mobility with  $T_s$  were reported. As a consequence, the effect of  $T_s$  on the growth and quality of the films is still unclear. In this communication, some unexpected influence of  $T_s$  on the growth of pentacene films was reported and explained by using classic film growth theories while considering the weak interaction at the organic/inorganic interface, and a modified bimodal growth mechanism at elevated  $T_s$  was proposed to explain both the out-of-plane and the in-plane grazing incidence x-ray diffraction patterns of the same films.

<sup>3</sup> Author to whom any correspondence should be addressed.

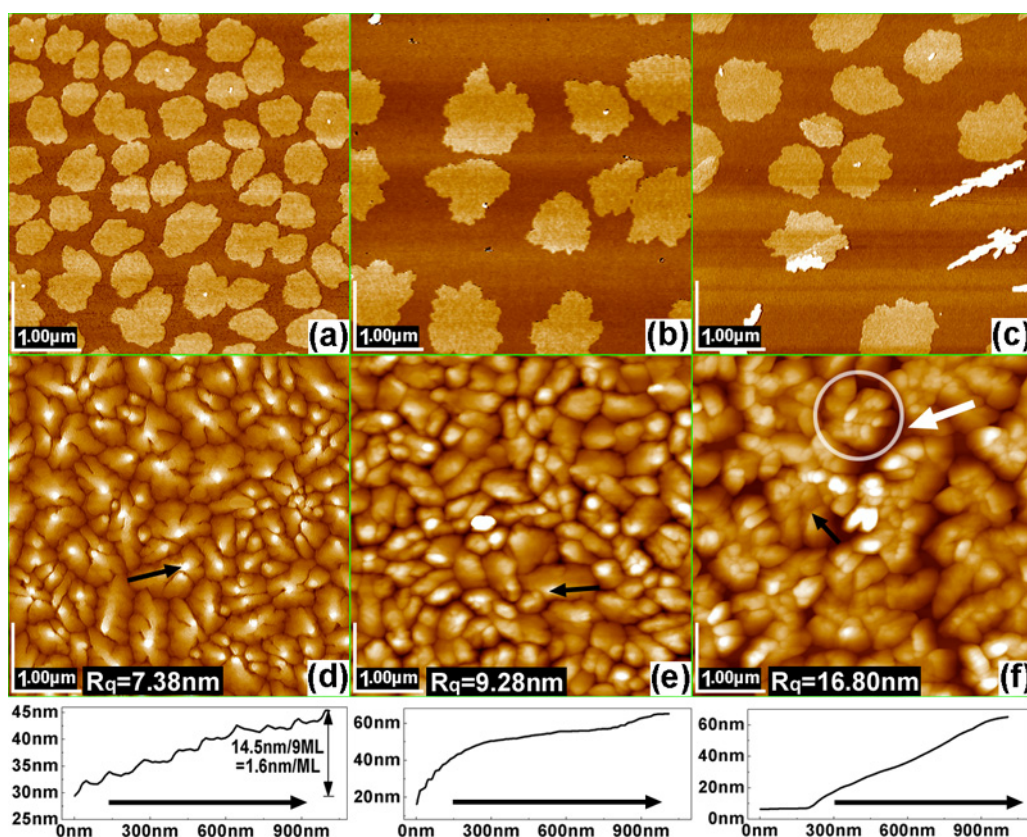


**Figure 1.** AFM images: (a) 0.6 ML deposited at RT; (b) 0.6 ML deposited at 50 °C; (c) 0.6 ML deposited at 60 °C; (d) 30 nm deposited at RT; (e) 30 nm deposited at 50 °C; (f) 30 nm deposited at 60 °C. The white circle in (f) indicates a group of aggregated islands, and the white arrow in the image indicates the void caused by the coarsening behavior. The RMS roughness and the height profiles (along the black arrows in the AFM images) of 30 nm samples are also illustrated.

## 2. Experiment methods

Pentacene powder was used as received from Aldrich Chemical to grow films by molecular beam deposition in a vacuum with a well controlled pressure of  $\sim 5 \times 10^{-5}$  Pa. Heavily doped n-type silicon wafers with a 300 nm thermally grown SiO<sub>2</sub> layer (average roughness <1 nm) produced by KST Corp. were used as the substrates, which were cleaned by acetone just before use. The substrates were heated with a tungsten wire and the  $T_s$  was measured by attaching a Chromel–Alumel thermocouple head on the substrate edge. Due to the difficulty in precisely controlling and detecting the surface temperature during vacuum deposition, the actual substrate surface temperature might be slightly higher than the detected values. All samples were deposited at the same nominal deposition rate of  $\sim 0.6$  nm min<sup>-1</sup>. The deposition rate and the film thickness were monitored with a well calibrated quartz crystal microbalance (QCM) kept at room temperature (not heated by the tungsten wire). The distance of the Knudsen cell to the sample surface is 20 cm. Film morphology was observed by a JEOL JSPM-5200 atomic force microscope (AFM) operated at non-contact mode. High precision out-of-plane x-ray diffraction (XRD) and grazing incidence x-ray diffraction (GIXD) profiles were obtained using an ATX-G thin film diffractometer with a five-axis goniometer.

## 3. Results and discussion

The AFM images of the pentacene films with a nominal thickness of 0.6 ML (1 ML = 1.54 nm) deposited at room temperature (RT = 26 °C), 50 °C and 60 °C are shown in figures 1(a), (b) and (c), respectively. The AFM images of the 30 nm thick pentacene films deposited at RT, 50 °C and 60 °C are shown in figures 1(d), (e) and (f), respectively. The height profiles of the 30 nm samples are also illustrated in figure 1 below the corresponding AFM images. The  $T_s$  dependence of grain coverage for the 0.6 ML films and the  $T_s$  dependence of grain size (circular-area-equivalent-diameter averaged from three AFM images) for both the 0.6 ML and the 30 nm films derived from the AFM images are shown in figure 2. For the 0.6 ML films, increased  $T_s$  enlarges the grains and slightly reduces the coverage. Since the same nominal deposition rate of  $\sim 0.6$  nm min<sup>-1</sup> (detected by the QCM without heating) was used for all samples, the reduced coverage with  $T_s$  must result from a slightly enhanced molecule desorption, which is around 38% judging from the AFM coverage of the 60 °C sample and much less (<30%) judging from the height histogram. Interestingly, some star-shaped islands appear in figure 1(c), which indicate a thermally induced roughening and three-dimensional growth. This can explain the slightly smaller grain size at  $T_s = 60$  °C than that at  $T_s = 50$  °C. According to the experiential relationship  $N = F^p/D^q$ , where  $p$  and  $q$

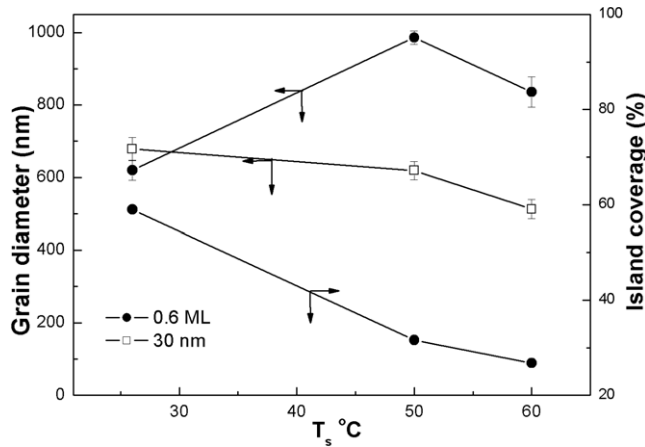


**Figure 2.**  $T_s$  dependence of grain size and island coverage (for 0.6 ML films).

are positive and are dependent on the nucleation mechanisms, and  $F$  is the deposition rate [12], the nucleus density  $N$  decreases with diffusion coefficient  $D$ .  $D$  is determined by  $T_s$  according to the relationship  $D = D_0 \text{Exp}(-E_a/kT_s)$ , where  $E_a$  is the diffusion energy barrier. Therefore, the increased grain size can be attributed to the improved surface diffusion with increasing  $T_s$ . However, the reduced coverage together with the island aggregation make it difficult to quantitatively characterize the effect of  $T_s$  on the grain size. For the 30 nm films, with increasing  $T_s$  the typical dendritic grain geometry transforms to a compact one, and the corresponding height profiles reveal that the layered grains change to clusters without a discernible terrace. Note that the decreased island size of the 30 nm films is inconsistent with the enlarged monolayer grains in 0.6 ML films. This is rather different from previous observations [8, 9, 11, 13, 14], and it is also unexpected considering the improved diffusion. Interestingly, from a closer check of the morphology of the film deposited at 60°C shown in figure 1(f), one can find a coarsening-like behavior. Namely, the islands tend to aggregate together, though they do not completely coalesce, forming groups of islands and leaving bare substrate voids. An island aggregation and the surrounding voids are indicated, respectively, by the white circle and the white arrows in figure 1(f). Also, the increased root mean square roughness ( $R_q$ ) with  $T_s$  shown in the AFM images of the 30 nm films reveals a thermally induced roughening. These results imply a gradual transition from the normal layer-plus-island (Stranski–Krastanov) growth to a three-dimensional island mode (Volmer–Weber) growth with increasing  $T_s$ .

According to the diffusion-limited-aggregation (DLA) model, the general fractal growth of pentacene with dendritic grain shape is due to the ‘island-corner barrier effect’ [15, 16], since an ad molecule on the substrate surface has to lower its coordination in crossing a grain edge corner in order to arrive at an energetically more stable site. Also, it is not difficult to understand that an increase in  $T_s$  should enhance the molecule diffusion along the grain edge and destabilize those edge corner molecules during deposition [16, 17]. Therefore, grains with a more compact shape and a lower total boundary free

energy are generally favored at elevated temperatures [16–18]. Considering the amorphous nature of the  $\text{SiO}_2$  substrate, the three-dimensional growth may not be simply ascribed to the accumulated strains as for the epitaxial growth of inorganic films on a crystalline surface. A recent thermodynamic analysis of the growth of small organic molecules on an inert substrate shows that three-dimensional growth is favored at a higher substrate temperature due to the lower supersaturation (the difference between the chemical potential of the vapor phase and the solid phase of the crystal) [19]. However, for explaining the coarsening behavior and the decreased grain size at a higher substrate temperature, influence of the kinetic processes, such as desorption and interlayer and intralayer diffusion should also be considered, since during deposition the system is not in an equilibrium status. The driving force of the coarsening-like behavior should be the minimization of the total free energy of each island, as the aggregated islands have a lower boundary free energy [16]. Investigation on inorganic films indicates that two mechanisms are responsible for the coarsening: atom exchange between islands due to evaporation and condensation, and island diffusion and coalescence [20, 21]. Thus, coarsening may be accelerated at a higher temperature, no matter which mechanism is responsible here. It is not difficult to understand that the interaction between the organic pentacene molecules and the inorganic  $\text{SiO}_2$  surface is weaker than the interaction between different pentacene layers, though both are van der Waals interactions, and a pentacene molecule can be more tightly bound on a pentacene layer than on the  $\text{SiO}_2$  surface. Therefore, we may presume that the uncovered first ML molecules in contact with the substrate may more easily desorb (molecule desorption is a basic process in film growth, and it may be accelerated by temperature) compared to the molecules in the upper layers during deposition. Actually, the desorption ratio derived from the AFM histogram of the 30 nm films is negligible compared to the desorption ratio of the 0.6 ML film (<30% at  $T_s = 60^\circ\text{C}$ ). This is consistent with the preferential desorption of the first monolayer molecules. These are consistent with a recent study on pentacene film morphology evolution [22], which indicates the possibility of molecular desorption from the first ML (see figure 4(a)). Namely, we may presume that the kinetic reason for the decreased island size with increasing  $T_s$  is the promoted desorption of the uncovered molecules in the first ML, while the thermodynamic cause of the decreased island size is the three-dimensional growth. Both factors prevent lateral growth, leading to decreased island size. Further work is needed to clarify the details.

The out-of-plane XRD and GIXD profiles of the 30 nm films are shown in figures 3(a) and (b), respectively. It should be noted that, the diffraction intensity of highly orientated films is very sensitive to the x-ray incidence angle. Hence, to make an accurate comparison, here, highly reproducible XRD scans were carried out after a precise sample position adjustment with a five-axis goniometer. The procedure is similar to that used for the GIXD measurements. Agreeing well with previous studies, both XRD and GIXD profiles reflect an increased fraction of the ‘bulk phase’ with increasing  $T_s$  [5–7]. This indicates that the ‘bulk phase’ is thermodynamically

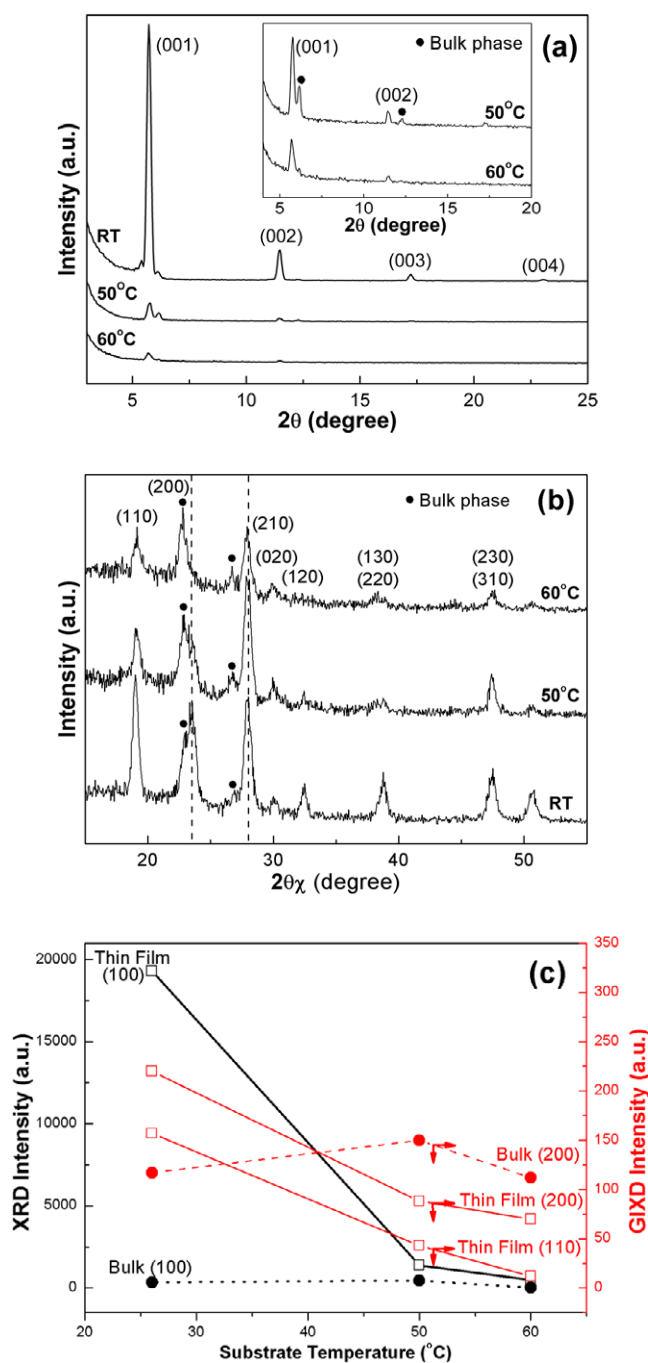


**Figure 3.** (a) XRD profiles of the 30 nm pentacene films deposited at different temperatures. The inset shows the magnified XRD profiles; (b) GIXD profiles of the 30 nm pentacene films deposited at different temperatures; (c) comparison of the intensity of the thin film phase (100) and the bulk phase (110, 200) signals. The dashed lines in (b) denote the (200) and (210) plane diffraction position of the thin film phase.

more stable than the ‘thin film phase’, although the latter is kinetically favored at the nucleation stage due to its lower (001) plane surface energy [5]. Surprisingly, as an analog to the decreased grain size, a substantially decreased diffraction intensity with  $T_s$  can be seen in figures 3(a) and (b), especially the former. Note that the diffraction intensity decrease is too sharp to be accounted for by the negligible desorption of the

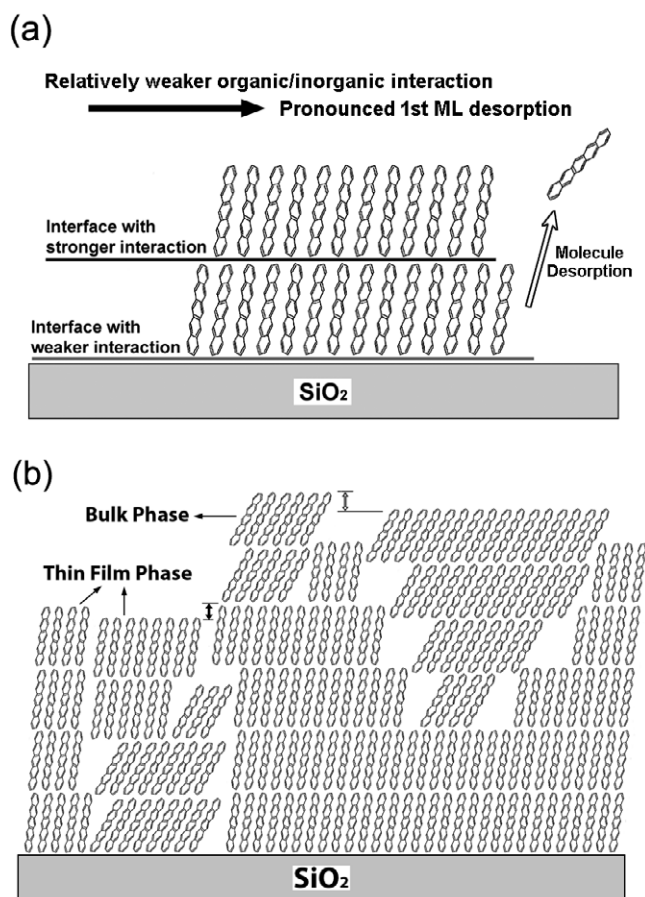


**Figure 4.** (a) Schematic illustration of the pronounced molecule desorption in the first ML due to the different interface interactions; (b) schematic illustration of the modified bimodal growth mechanism at elevated  $T_s$  with the two phases nucleating on each other. The filled and open double arrows, respectively, indicate the height difference between thin film phase and bulk phase crystallites.

same 30 nm samples. Therefore, the decreased XRD intensity should reflect a substantially decreased crystallinity, which can not be explained by the inorganic film growth theories [16, 23], and is different from the expectation for growth of organic films [1, 8]. Due to the large size, anisotropic shape and weak van der Waals interaction of organic molecules, their crystallization is much more complicated than that of inorganic films. Thus, to give a tentative explanation, we may postulate that the significantly enhanced kinetic molecular processes with  $T_s$ , such as surface diffusion (as shown in figure 1), interlayer mass transport [16, 17] and molecule desorption, favor the formation of various defects and hinder the ordered molecular packing. Further work is necessary for elucidating the details. It needs to be clarified that the ‘grain size’ derived by AFM reflects the grain geometry, which is different from the ‘coherent diffraction domain size’ for both XRD and GIXD. The coherent diffraction domain size for XRD is the vertical size along the surface normal, while the horizontal domain size for GIXD is generally much smaller than the AFM grain size. Thus, neither the XRD nor the GIXD peak width could reflect the grain size.

Interestingly, both XRD and GIXD profiles reveal that the nucleation of the bulk phase has started at RT, although its

signals are very weak. This temperature is significantly lower than the previously reported 90 °C value for a 30 nm film [7]. To see the structural change more clearly, the intensities of the thin film phase (100) and the bulk phase (110, 200) signals are compared in figure 3(c). One can see that while the intensities of the thin film phase signals (the hollow square) in both diffraction profiles decrease significantly with  $T_s$ , the bulk phase signals (the filled circle), particularly those of the GIXD patterns, are relatively much more constant. This implies that the widely reported increase of the bulk phase crystallite quantity with  $T_s$  [5, 7, 13, 24] may be actually a reflection of a reduced thin film phase crystallite quantity, while the bulk phase quantity is almost temperature independent. Furthermore, from a closer examination of figure 3(c) one can find that, in sharp contrast to the substantially decreased XRD intensity of the thin film phase with increasing  $T_s$ , the GIXD intensity of this phase only shows a slight decrease with  $T_s$ . Apparently, this discrepancy can not be simply explained by a decreased crystallinity, or by a change in the relative ratio of the two phases. According to a recently developed bimodal growth mechanism of pentacene [6], the bulk phase crystallites nucleate on different layers of the thin film phase crystallites with increasing film thickness. Consequently, due to the different (001) lattice spacing of the thin film phase (1.54 nm) and the bulk phase (1.45 nm), the crystallites of the latter phase formed on different thin film phase layers may show a varied (001) plane position, and hence do not scatter in phase for the out-of-plane diffraction, leading to a weak bulk phase XRD intensity with increasing thickness, while the in-plane GIXD peaks are largely unaffected. However, the present observations indicate that this mechanism needs to be modified at elevated temperatures. Namely, the thin film phase crystallites might also nucleate on the bulk phase crystallites, and the corresponding mixed bimodal growth is illustrated by figure 4(b). With increasing  $T_s$  more thin film phase crystallites start to nucleate on the bulk phase layers. Thus, their (001) planes with random height difference (as indicated by the double arrow in figure 4(b)) may not scatter in phase for the corresponding out-of-plane XRD signals, while the in-plane GIXD signals are not significantly affected. Consequently, a much sharper decrease of XRD intensity than in the GIXD intensity of the thin film phase signals was observed with increasing  $T_s$ .

In summary, the unexpected decrease in grain size with increasing  $T_s$  was attributed to a pronounced desorption of the uncovered first monolayer molecules as a consequence of the weak interaction at the pentacene/SiO<sub>2</sub> interface as well as a two-dimensional to three-dimensional growth transition. The coarsening-like behavior and dendritic to compact grain geometry transition were explained by using classic film growth theories. A modified mixed bimodal growth

mechanism was proposed to explain both the XRD and GIXD patterns. The presented results may contribute to a better understanding of organic thin film growth.

## Acknowledgments

This research is supported by a Grant-in-Aid for Scientific research from MEXT of Japan (14GS0207). One of the authors (Guo) is also grateful to the Japan Society for the Promotion of Science (JSPS) and the Bai Ren project of the Chinese Academy of Sciences for their financial support.

## References

- [1] Ruiz R, Choudhary D, Nickel B, Toccoli T, Chang K C, Mayer A C, Clancy P, Blakely J M, Headrick R L, Iannotta S and Malliaras G G 2004 *Chem. Mater.* **16** 4497
- [2] Fritz S E, Martin S M, Frisbie C D, Ward M D and Toney M F 2004 *J. Am. Chem. Soc.* **126** 4084
- [3] Conrad B R, Gomar-Nadal E, Cullen W G, Pimpinelli A, Einstein T L and Williams E D 2008 *Phys. Rev. B* **77** 205328
- [4] Meyer zu Heringdorf F J, Reuter M C and Tromp R M 2001 *Nature* **412** 517
- [5] Kakudate T, Yoshimoto N and Saito Y 2007 *Appl. Phys. Lett.* **90** 081903
- [6] Mayer A C, Kazimirov A and Malliaras G G 2006 *Phys. Rev. Lett.* **97** 105503
- [7] Bouchoms I P M, Schoonveld W A, Vrijmoeth J and Klapwijk T M 1999 *Synth. Met.* **104** 175
- [8] Schreiber F 2004 *Phys. Status Solidi a* **201** 1037
- [9] Jin S H, Jung K D, Shin H, Park B G and Lee J D 2006 *Synth. Met.* **156** 196
- [10] Dimitrakopoulos C D, Brown A R and Pomp A 1996 *J. Appl. Phys.* **80** 2501
- [11] Lee J, Kim J H and Im S 2004 *J. Appl. Phys.* **95** 3733
- [12] Pimpinelli A, Villain J and Wolf D E 1992 *Phys. Rev. Lett.* **69** 985
- [13] Yagi I, Tsukagoshi K and Aoyagi Y 2004 *Thin Solid Films* **467** 168
- [14] Knipp D, Street R A, Volkel A R and Ho J 2003 *J. Appl. Phys.* **93** 347
- [15] Witten T A and Sander L M 1981 *Phys. Rev. Lett.* **47** 1400
- [16] Zhang Z Y and Lagally M G 1997 *Science* **276** 377
- [17] Brune H 1998 *Surf. Sci. Rep.* **31** 121
- [18] Hwang R Q, Schroder J, Gunther C and Behm R J 1991 *Phys. Rev. Lett.* **67** 3279
- [19] Verlaak S, Steudel S, Heremans P, Janssen D and Deleuze M S 2003 *Phys. Rev. B* **68** 195409
- [20] Thomas R M, Greg M and Metiu H 1999 *J. Appl. Phys.* **110** 12151
- [21] Pai W W, Swan A K, Zhang Z Y and Wendelken J F 1997 *Phys. Rev. Lett.* **79** 3210
- [22] Shi J and Qin X R 2008 *Phys. Rev. B* **78** 115412
- [23] Venables J A, Spiller G D T and Hanbrcken M 1984 *Rep. Prog. Phys.* **47** 339
- [24] Mattheus C C, Dros A B, Baas J, Oostergetel G T, Meetsma A, de Boer J L and Palstra T T M 2003 *Synth. Met.* **138** 475